current flow in the inhomogeneous but isotropic semiconductor is $qD(r)\nabla n(r)$. Although it would appear desirable to formulate the current flow equations in terms of the conductivity parameter as in (1), such a formulation is not a logical development for materials with point to point variations of the transport parameters such as are caused by a large spatial variation of the impurity concentration.

References

[1] H. C. Lin, J. C. Ho, R. R. Iyer, and K. Kwong, "Complementary MOS-bipolar transistor structure," *IEEE Trans. Electron Devices*, vol. ED-16, Nov. 1969, pp. 945–951.
[2] S. Wang, *Solid-State Electronics*. New York: McGraw-Hill, 1966, ch. 4.
[3] J. R. A. Beale, "The calculation of transit time in junction transistors when the mobilities are not constant," *Proc. IRE* (Corresp.), vol. 48, July 1960, p. 1341.
[4] J. M. Ziman, *Electrons and Phonons*. New York: Oxford University Press, 1960, ch. 7.

Transition Region Capacitance of Diffused p-n Junctions

BASANT R. CHAWLA, MEMBER, IEEE, AND HERMANN K. GUMMEL, SENIOR MEMBER, IEEE

Abstract—**The classical capacitance–voltage relations based on abrupt space-charge edge approximations, while adequate at large reverse bias, do not adequately describe the capacitance near zero bias. This paper presents explicit capacitance–voltage relations valid near zero bias for linearly graded and exponential-constant profiles. For linearly graded junctions, the intercept in a $1/C^3$ versus voltage plot is shown to be well approximated by the "gradient voltage" defined by**

$$V_g = \frac{2}{3}\frac{kT}{q}\ln\frac{a^2\epsilon kT/q}{8qn_i^3}.$$

Also presented is an accurate numerical technique for machine computation of the transition region capacitance for any doping profile. Explicit relations obtained by dimensional considerations and curve fitting on numerical solutions are free of singularities, hence useful in computer-aided device design and doping profile determination.

I. Introduction

THE classical capacitance–voltage relationships for steps and linearly graded p-n junctions form useful tools for evaluating impurity concentration profiles in semiconductors [1]. These relations, however, have certain limitations. The technique based on the so-called "C square-root V" relation for step junctions assumes that one side of the junction is much more heavily doped than the other. This limits its application to alloyed or very shallow diffused junctions. Furthermore, since the above relations were derived by making an abrupt space-charge edge (ASCE) approximation, i.e., that the material is either completely depleted of mobile carriers or is completely neutral, it is acceptably accurate only at large reverse bias. This limits the evaluation of the doping profile to the region away from the junction. To "probe" the neighborhood of the junction, the bias range of interest is from low reverse bias to forward bias. It is exactly in this range that the classical C square-root V relation fails to describe the junction accurately. Analyses that do not assume the ASCE approximation and describe p^+n step junctions in this bias range have recently been presented by Gummel and Scharfetter [2], Chang [3], and Kleinknecht [4]. Note that the capacitance in our discussion is the transition region capacitance only.

The conventional doping profile analysis is thus useful only for highly asymmetrical step junctions. For junctions with comparable doping concentrations on both sides, a unique profile on one side cannot be determined without any a priori knowledge of the doping profile of the other side. For gradual doping transition and low bias, such junctions, however, may be considered linear-graded for which, with the ASCE approximation, $d(1/C^3)/dV$ is approximately proportional to the concentration gradient. Treatments of linearly graded junctions not restricting to abrupt approximation have been given by Morgan and Smits [5], Sah [6], Kennedy and O'Brien [7], and Nuyts and Van Overstraeten [16].

In practice, most diffused junctions with error-function, Gaussian, or similar doping profiles lie on an intermediate level between highly asymmetrical and linear-graded junctions. Lawrence and Warner [8] have given curves applicable for diffused junctions with error-function and Gaussian doping profiles, which relate background concentration, junction depth, and "total voltage," where total voltage is the applied

Manuscript received October 2, 1970.
The authors are with Bell Telephone Laboratories, Inc., Murray Hill, N. J.

voltage minus the so-called "built-in voltage." These curves are very useful for large reverse-bias voltages. However, difficulties arise if the curves are to be used near zero bias.

In the neighborhood of zero bias, the total voltage is not well defined. For example, at zero bias, the total voltage, according to the definition in classical C–V relationships and the definition used by Lawrence and Warner [8], would be the negative of the built-in voltage. For highly asymmetrical step junctions, it has been shown [2]–[4] that, at zero bias, the total voltage differs significantly from the negative of the built-in voltage. In this paper, we shall develop the concept of a quantity termed "offset voltage," which depends on doping parameters and to a lesser extent on applied voltage. The total voltage at zero bias is then given by the negative of the offset voltage at zero bias. The basic concepts underlying the definitions of the transition-region capacitance, as distinguished from the diffusion capacitance, and of the offset voltage are presented in Section II.

In Section III we make the abrupt space-charge edge approximation to obtain an analytical expression for the capacitance–voltage relationship for an exponential-constant doping profile. Such profiles provide a realistic approximation for many diffused p-n junction profiles.

In Section IV we present a numerical technique, not involving the ASCE approximation, for computing transition region capacitance for arbitrary doping profiles at reverse as well as forward bias. The technique is based on an operational definition described in Section II.

In Section V we consider the offset voltage for linearly graded junctions. Based on dimensional considerations, an analytical expression is found which is termed "gradient voltage" and is shown to be an excellent approximation to the offset voltage.

Section VI contains the application of the technique of Section IV to the doping profile analysis of diffused p-n junctions and computer-aided analysis of circuits containing semiconductor components fabricated by diffusion technology. First we find offset voltage values for a set of applied voltages and a set of doping parameters for exponential-constant doping profile. An analytical expression is then fitted to the above values, and used in plotting constant capacitance curves in doping parameter space for different bias values.

II. Basic Concepts

Differential capacitance is conventionally defined as the derivative of stored charge with respect to voltage. This definition will be used in this paper. The total capacitance of p-n junction diodes, or of devices containing p-n junctions, is usually considered as consisting of two components, transition-region capacitance and diffusion capacitance.

Qualitatively these two components are easily distinguished. Transition-region capacitance is associated with differential charge storage at the edges of the depletion region. It is the dominant capacitance for reverse-biased junctions. The transition-region capacitance is independent of frequency up to very high frequencies. The admittance of a reverse-biased p-n junction diode at low frequencies may differ from its capacitive susceptance due to series resistance. If the series resistance is low, the diode exhibits a large value of the quality factor Q. Transition-region capacitance depends only on the doping profile in the depletion region and its immediate vicinity. Diffusion capacitance, on the other hand, is associated with storage of carriers in regions adjacent to the depletion region. It is significant only for forward-biased junctions. Diffusion capacitance depends on the structure of the diode as a whole; it depends on recombination properties (lifetime) and may (for short diodes) depend on the nature of the contacts. Diffusion capacitance is strongly frequency-dependent. At high frequencies the diffusion capacitance may become negative (e.g., Misawa [9]), giving rise to inductive effects. When in a p-n junction diode the diffusion capacitance is dominant over the transition region capacitance, the quality factor Q of the diode is always low.

While a qualitative distinction of transition-region and diffusion capacitance is easily made, a quantitative separation becomes problematic. With modern techniques of analysis [10], [11], p-n junction devices may be analyzed on the basis of transport, continuity, and space-charge balance equations; terminal characteristics including all the capacitive effects are reproduced by such calculations without the need of classification of capacitance into various categories. On the other hand, for the construction of compact device models, it is very desirable to have available simple, quantitative models of charge storage effects having reasonable accuracy.

Existing descriptions of transition-region capacitance are well developed and quite adequate for reverse-biased junctions. For heavily forward-biased junctions, the transition-region capacitance is typically negligibly small in comparison with diffusion capacitance, and is thus of minor interest. It is for forward bias of such magnitude that the transition-region capacitance is comparable to, or less than, diffusion capacitance that compact representations of transition-region capacitance are not readily available.[1] This range of bias is of great practical importance in bipolar transistors, since the highest frequency response is obtained when the emitter-junction forward bias is such that transition-region and diffusion capacitance are roughly comparable.

In the present paper we propose an operational

[1] A model of transition-region capacitance, based in part on the present work, has recently been reported by Poon and Gummel [12].

definition of transition-region capacitance that has the following features.

1) For reverse-biased junctions it coincides with the conventional definition of transition region capacitance.

2) It gives a finite value of transition-region capacitance for any bias, especially for forward bias equal to or larger than the built-in voltage.

3) It selects charge storage associated only with carriers in the immediate vicinity of the p-n junction, in accordance with the qualitative concept of transition-region capacitance.

4) Transition-region capacitance computed according to the definition depends on the doping profile only, not on recombination properties.

We define the transition-region capacitance as the change in the *net* hole charge per change in voltage. The *net* hole concentration is defined as the difference between the *actual* hole concentration and the hole concentration which would exist if space-charge neutrality prevailed throughout the structure. We shall refer to the latter quantity as *space-charge neutral hole concentration*. Note that there will be an equal change in the *net* electron charge and we could have defined the transition-region capacitance with respect to changes in the net electron charge.

Let us now consider the dependence of the transition-region capacitance on the applied voltage. Consider a step junction with uniform doping on the two sides. We could express the transition-region capacitance for this junction in terms of the capacitance given by the classical C square-root V relation, except that difficulties arise when the applied voltage is equal to the so called built-in voltage, since the capacitance given by that relation then goes to infinity. Alternatively, we can use the same mathematical form, but replace the built-in voltage by a more appropriate quantity. This alternative looks more attractive and is pursued in the following.

Let us consider a junction with an arbitrary doping profile. Then using the ASCE approximation, i.e., assuming the mobile carrier density at the edge of the depletion region to be zero, the electric field in the depletion region can be written as

$$E(X) = E_0 + \int_0^x \frac{q}{\epsilon} N(x)dx \tag{1}$$

where $N(x)$ is the impurity concentration, E_0 is the field at the metallurgical junction $x=0$, and other quantities have the conventional meaning.

The *total voltage* is then defined as the integral of the electric field across the depletion region:

$$V_t = \int_{x_l}^{x_r} E(x)dx \tag{2}$$

where x_l and x_r are, respectively, the left and the right edge of the depletion region, i.e., the position where the electric field as given by (1) goes to zero.

Now, since the depletion-region capacitance is proportional to the inverse of the width $W=x_r-x_l$, (2) can be stated as

$$V_t = F(C_a) \tag{3}$$

where C_a is the capacitance per unit area found by using the ASCE approximation and depends on the doping profile. The exact capacitance C_e, however, is obtained by removing the above approximation and hence will in general differ from C_a. Replacement of C_a in (3) by C_e will therefore yield a different value for the total voltage. We define this new total voltage as the difference between the *applied voltage* and a quantity *offset voltage*.

$$V_{\text{app}} - V_{\text{offset}} \equiv F(C_e). \tag{4}$$

The *offset voltage* is therefore defined as

$$V_{\text{offset}} \equiv V_{\text{app}} - F(C_e), \tag{5}$$

and is a function of applied voltage and the doping parameters. The offset voltage is thus an exact quantity in that when used in place of built-in voltage in the standard $C-V$ relations, one obtains "exact" transition-region capacitance at all applied voltages. In this respect, the built-in voltage can be regarded as a first-order approximation to the offset voltage. Higher order approximations, based on dimensional considerations and the numerical technique of Section IV, are presented in this paper for linearly graded and exponential-constant profiles.

III. Exponential-Constant Profile—ASCE Approximation

A first-order calculation of the transition-region capacitance can be performed by making the abrupt space-charge edge approximation. Let us consider an exponential-constant doping profile described by

$$N_B = N(1 - e^{-x/L}), \tag{6}$$

and let the electric field at the metallurgical junction $x=0$ be E_0. Then, using the ASCE approximation and Poisson's equation, we obtain

$$E(x) = E_0 + \frac{qNL}{\epsilon}\left(\frac{x}{L} + e^{-x/L} - 1\right). \tag{7}$$

Denoting by $\xi \equiv x/L$ the normalized distance and by ξ_L and ξ_R the values of ξ for which the electric field goes to zero, and letting $w=\xi_R-\xi_L$ be the width of the depletion region in units of the characteristic length L, from (7) we obtain

$$e^{-\xi_R} = \frac{w}{e^w - 1}. \tag{8}$$

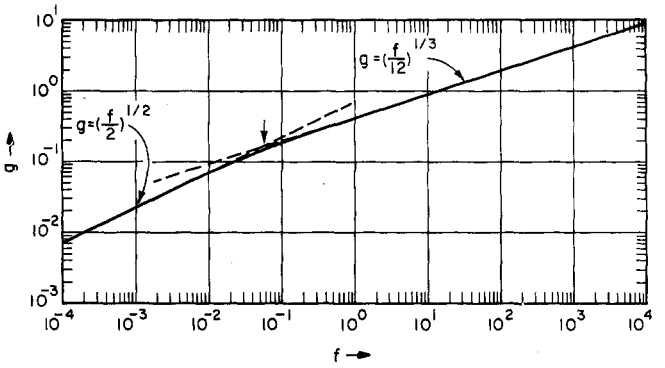

Fig. 1. The function g versus f (10).

Denote by V_t the total voltage as the integral of the field

$$V_t = L\int_{\xi_L}^{\xi_R} E(\xi)d\xi = -\frac{qNL^2}{\epsilon f\left(\frac{1}{w}\right)}, \tag{9}$$

where the function f of argument g is defined by

$$f(g) \equiv \frac{2g^2}{\coth\left(\frac{1}{2g}\right) - 2g}. \tag{10}$$

Equation (9) together with (10) has recently been reported in the literature [13]. Now, under the ASCE approximation the capacitance per unit area C is defined as

$$C = \frac{\epsilon}{wL} \tag{11}$$

whence

$$\frac{CL}{\epsilon} = \frac{1}{w} = g\left(\frac{qNL^2}{\epsilon(-V_t)}\right), \tag{12}$$

where $g(f)$ is the inverse function to $f(g)$ (10). A plot of g versus f is shown in Fig. 1.

Equation (12) is a general, analytic relation between N, L, C, and V_t. As shown in Fig. 1, the function $g(f)$ approaches $\sqrt{f/2}$ for small arguments and $(f/12)^{1/3}$ for large arguments. Thus, for $CL/\epsilon \ll 1$, (12) yields

$$C^2 = \frac{q\epsilon N}{2(-V_t)}, \tag{13}$$

and for $CL/\epsilon \gg 1$, (12) yields

$$C^3 = \frac{q\epsilon^2(N/L)}{12(-V_t)}. \tag{14}$$

Equations (13) and (14) are the standard expressions for the capacitance of the asymmetric step junction and the linear-graded junction, respectively, where V_t is the difference between the applied voltage and the so-called built-in voltage. For Gaussian and error-function complement diffusion profiles having a surface concentration N_s and junction depth x_j, the equivalent exponential decay length L at the metallurgical junction can be given approximately by

$$L \simeq \frac{l^2}{2x_j} \tag{15}$$

where l is the characteristic length of the diffusion profile to be determined as follows.

For Gaussian profiles

$$l^2 = \frac{x_j^2}{\ln(N_s/N)}, \tag{16}$$

and for complementary error function profiles

$$N = N_s \operatorname{erfc}\left(\frac{x_j}{l}\right). \tag{17}$$

Equation (12) is then the equivalent of Lawrence–Warner curves [8].

A more exact relation between the capacitance, doping parameters, and the bias voltage can now be obtained by incorporating correction terms in (9), based on exact calculations using the numerical technique discussed in the following section.

IV. Numerical Solution

The basic concepts for calculating the transition-region capacitance were set forth in Section II. In the numerical technique described here, the hole quasi-Fermi level (in units of kT/q) ϕ_p is assumed to be spatially constant from the p-region contact up to and through the junction, and likewise, the electron quasi-Fermi level ϕ_n is assumed to be spatially constant from the n-region contact up to and through the junction region. This assumption is excellent for reverse bias. However, at forward bias the current flow causes a significant bending of the quasi-Fermi levels, and hence the assumption loses validity insofar as the calculation of current is concerned. But it does not cause any serious error in calculating the transition region capacitance. This has been verified by comparing results with those obtained by a more accurate analysis which takes into account the bending of the quasi-Fermi levels. The above assumption is made for reasons of economy in computation; it is also consistent with the operational definition (feature 4 of Section II). Furthermore, it is assumed that all the donors and acceptors are fully ionized and that the amount of stored charge in deep states is negligible.

Let us now denote by p_s and n_s the space-charge neutral hole and electron concentrations corresponding

to space-charge neutrality. In terms of the quasi-Fermi levels, they are given by

$$p_s = n_i e^{\phi_p - \psi_s} \tag{18}$$

$$n_s = n_i e^{\psi_s - \phi_n} \tag{19}$$

where the space-charge neutral electrostatic potential ψ_s is adjusted so that $p + N_E = n$, whence

$$\psi_s = \phi_p - \ln\left[\left\{\left(\frac{N_E}{2n_i}\right)^2 + \exp(\phi_p - \phi_n)\right\}^{1/2} - \frac{N_E}{2n_i}\right]$$

$$= \phi_n + \ln\left[\left\{\left(\frac{N_E}{2n_i}\right)^2 + \exp(\phi_p - \phi_n)\right\}^{1/2} + \frac{N_E}{2n_i}\right] \tag{20}$$

with N_E as the effective doping and the quantities p_s, n_s, and ψ_s as functions of distance.

Next we denote by p_n the net hole concentration as the difference between the actual hole concentration p and space-charge neutral concentration p_s. Similarly, we denote by n_n the net electron concentration as the difference between the actual electron concentration n and space-charge neutral concentration n_s. Denoting by y the difference between the actual electrostatic potential ψ (in units of kT/q) and the space-charge neutral potential ψ_s,

$$y \triangleq \psi - \psi_s, \tag{21}$$

the net hole and electron concentrations may be expressed as

$$p_n \triangleq p - p_s = p_s(e^{-y} - 1) \tag{22}$$

and

$$n_n \triangleq n - n_s = n_s(e^{y} - 1). \tag{23}$$

Poisson's equation

$$\psi'' = -\frac{q}{\epsilon kT/q}(p_n - n_n) \tag{24}$$

can now be rewritten as

$$R \triangleq y'' + \frac{q}{\epsilon kT/q}[p_s(e^{-y} - 1) - n_s(e^{y} - 1)] + \psi_s'' \tag{25}$$

where R is required to be zero by (24).

Equation (25) may be solved iteratively for y. If R is not negligibly small everywhere for a given trial solution y, we seek an increment δy in y which reduces R. Linearizing (25) with respect to y, we find that δy must obey the equation

$$\delta y'' - \frac{q}{\epsilon kT/q}(p_s e^{-y} + n_s e^{y})\delta y = -R. \tag{26}$$

Consider now that a satisfactory solution y has been found for which the error R is acceptably small. We then seek the change in y per unit change in the normalized bias voltage $V \equiv \phi_p - \phi_n$. To obtain this, we first write the following equations which are equivalent to (18)–(20):

$$p_s n_s = n_i^2 e^{V} \tag{27}$$

$$p_s + N_E = n_s \tag{28}$$

from which it follows that

$$\delta p_s = \delta n_s = \frac{p_s n_s}{p_s + n_s}\delta V. \tag{29}$$

Consequently, from (18) and (19) we obtain

$$\delta\psi_s = \frac{1}{2}(\delta\phi_p + \delta\phi_n) + \frac{1}{2}\left(\frac{p_s - n_s}{p_s + n_s}\right)\delta V. \tag{30}$$

Using (29) and (30) in taking the variation of (25) with respect to V and defining the variation in y as Δy, we obtain

$$\Delta y'' - \frac{q}{\epsilon kT/q}(p_s e^{-y} + n_s e^{y})\Delta y + \left[\frac{q}{\epsilon kT/q}\frac{n_s p_s(e^{-y} - e^{y})}{(n_s + p_s)} + \frac{1}{2}\left(\frac{p_s - n_s}{p_s + n_s}\right)''\right]\delta V = 0. \tag{31}$$

Note that (26) and (31) are similar in form. They differ only in the "driving term," i.e., the error R in (26) and the term proportional to δV in (31). Boundary conditions are imposed such that the domain of the independent variable, i.e., the physical distance, ends in space-charge neutral regions on either side of the transition region, in which case the boundary conditions are that y and Δy must be zero at both ends. Note that whereas (26) is solved iteratively until R, and hence the change δy in y is acceptably small, (31) need be solved only once for a given bias value. Having found a solution Δy of (31) for $\delta V = 1$, the total change of net holes per unit area δP_N may be written as

$$\delta P_N = \int \delta p_n dx = \int \left\{\frac{n_s p_s}{p_s + n_s}(e^{-y} - 1) - p_s e^{-y}\Delta y\right\} dx, \tag{32}$$

and hence the capacitance per unit area is

$$C = \frac{q}{kT/q}\delta P_N. \tag{33}$$

The technique described above was formulated keeping in view the usage of a digital computer to obtain a solution. The function y is clamped to zero by boundary conditions, and it changes very little in the space-charge neutral regions. Hence by evaluating $(e^{\pm y} - 1)$ as $(\pm y + (y^2/2!) \pm (y^3/3!) + \cdots)$ for small y,

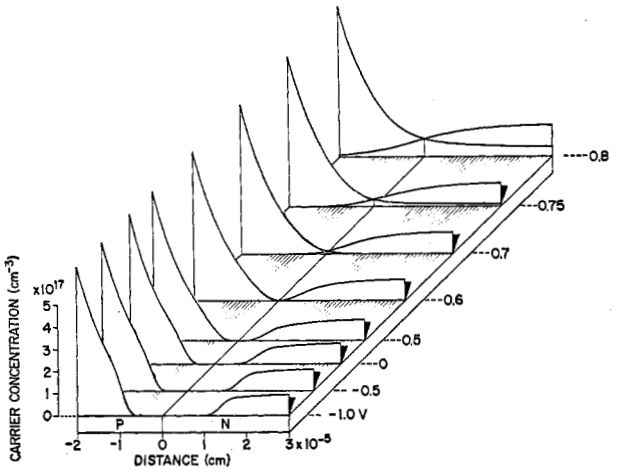

Fig. 2. Numerically computed actual hole and electron concentrations in a diode with a constant background concentration of 10^{17} cm^{-3} donors and a superposed exponential profile of acceptors with a characteristic length of 10^{-5} cm. Applied voltage is varied from -1 to 0.8 V.

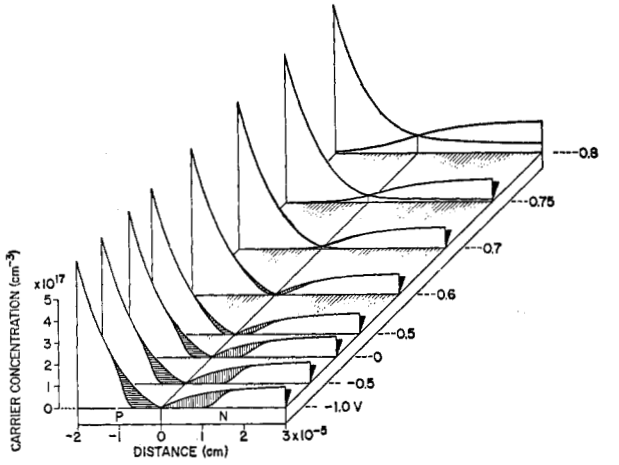

Fig. 3. For the same diode as in Fig. 2, actual carrier concentration (lower curve) and the carrier concentration corresponding to space-charge neutral solution in the diode (upper curve).

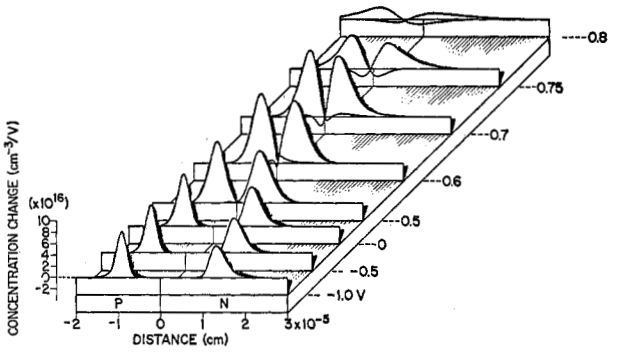

Fig. 4. For the same diode as in Fig. 2, the derivative of net carrier concentrations with respect to applied voltage.

we have effectively obtained a symbolic rather than a numerical cancellation of mobile and fixed charges with attendant benefits regarding roundoff errors. It is also of advantage that with only minor changes, the same computer program may be used to obtain actual carrier concentrations and their derivatives with bias.

As an example, the above technique is applied to a silicon p-n junction diode with doping profile consisting of a constant background concentration of 10^{17} cm^{-3} donors on which is superposed an exponential profile of acceptors with a characteristic length of 10^{-5} cm or 0.1 μ. The values of the physical constants used are $n_i = 1.5 \times 10^{10}$ cm^{-3}, $\epsilon = 10^{-12}$F/cm, and $kT/q = 0.02585$ V at room temperature.

Fig. 2 shows the computed actual hole and electron concentrations for applied voltages from -1 to 0.8 V. The ordinate is carrier concentration plotted on a linear scale, and the abscissa is distance. The total distance shown is 0.5 μ; the voltage increments are chosen not to be equal for better presentation. At reverse and zero bias, the carriers approach the doping values asymptotically on either side of the junction. Near the metallurgical junction we observe the depletion region where the carrier concentrations are negligible compared to the doping concentrations, and are indistinguishable from zero on the scales used. One can then define with reasonable accuracy the transition-region capacitance to be that of a plate capacitor with plate separation equal to the depletion layer width. The depletion layer width narrows as one goes from reverse bias to forward bias. At large forward bias we observe regions of overlapping hole and electron concentrations in what was the depletion region at reverse and zero bias. It is in this range that the parallel capacitor definition for transition region capacitance is no longer valid, requiring modifications embodied in this paper. Note also that even at the highest voltage shown, which exceeds the so-called built-in voltage, there are no singularities. Carrier concentrations, though rising, remain finite.

Fig. 3 shows the computed net carrier concentrations, depicted by crosshatched regions for bias values shown in Fig. 2. The upper curves in these regions correspond to *space-charge neutral* carrier concentrations, while the lower curves are the *actual* carrier concentrations shown in Fig. 2. For reverse and zero bias, the net carrier concentrations are negative, but at forward bias, both negative and positive net carrier concentrations prevail.

Fig. 4 shows the derivative of net carrier concentrations with respect to bias. At reverse bias the carrier concentration change is appreciable only in narrow regions, whereas at forward bias the change is spread over a wide region. The centers of gravity of these regions correspond to the location of equivalent capacitor plates. The capacitance per unit area equals exactly $C = \epsilon/w$, where w is the separation between the centers of gravity. At large forward bias, the regions of net carrier change overlap; hence the mental picture of

charge accumulation at the edges of a depletion region breaks down. It is, however, still true that the capacitance $C=\epsilon/w$ where w is the separation of the centers of gravity, but now the widths of the regions of net carrier change are larger than w. Clearly, at forward bias, w cannot be thought of as the width of a depletion region. Note that starting from large reverse bias, with more positive bias, the peaks move closer together and the areas under them increase, resulting in an increase of the capacitance. Beyond 0.7 V, however, the transition-region capacitance, as defined here, decreases. The *total* capacitance, which includes diffusion capacitance, however, increases since storage in the space-charge neutral regions is now enhanced. To reiterate, the important point is that total capacitance, as well as transition region capacitance, remain finite.

At 0.8 V, the last curve shown in Fig. 4, we observe that the net hole and net electron curves cross on the p side which is the more heavily doped side. Thus one may consider the junction to have moved over from its metallurgical location into the more heavily doped side. This has previously been pointed out by Ghosh [14].

V. Gradient Voltage—Linearly Graded Junctions

The numerical technique described in Section IV is useful for detailed device modeling. For circuit analysis programs which simultaneously handle many p-n junction devices, this approach would require too much memory and execution time to be practical. What is desirable is a compact analytical expression, free of singularities, which approximates the numerical data reasonably well. The concept of offset voltage developed in Section II is helpful here. In this section we shall show that for a linearly graded junction the offset voltage can be well approximated by a quantity which we shall term as "gradient voltage." The gradient voltage which is proportional to the logarithm of the doping gradient, is found by making use of some dimensional considerations, following the treatment of the linear-graded junction problem by Morgan and Smits [5]. In the following we derive the expression for the gradient voltage. Let us recast the differential equation (24) in terms of the normalized potential distribution in the junction, $Y(x)=(q/kT)\,[\psi-1/2(\phi_p+\phi_n)]$ as in [5], [21]:

$$\frac{d^2Y}{dx^2} = \sinh Y - Kx \tag{34}$$

where the parameter K in the present notation is

$$K = \frac{e^{-(3/4)U}}{\sqrt{8S}} = \exp\left\{-\frac{3}{4}\left[U + \frac{2}{3}\ln(8S)\right]\right\} \tag{35}$$

with

$$U \equiv \phi_p - \phi_n - \ln\left(\frac{N}{n_i}\right)^2, \qquad S \equiv \frac{qNL^2}{\epsilon kT/q}$$

and $N/L=a$ is the doping gradient for the junction.

The space-charge capacitance C in [5] is given by a normalizing capacitance C_0 multiplied by a function of K. The functional dependence is given in Table III of [5] in the column headed by $C\rho/C_0$ and we denote it here by $G(K)$:

$$C = C_\rho = C_0 G(K). \tag{36}$$

The quantity C_0 can be written in our notation as

$$\left(\frac{C_0 L}{\epsilon}\right)^3 = \frac{S}{64}, \tag{37}$$

and hence the normalized capacitance is

$$\frac{CL}{\epsilon} = \frac{S^{1/3}G(K)}{4}. \tag{38}$$

Now, since for large reverse bias (large K) the ASCE approximation is quite good and yields (see (14))

$$\frac{CL}{\epsilon} = \left(\frac{S}{-12\dfrac{q}{kT}V_t}\right)^{1/3}, \tag{39}$$

denoting $(kT/q\,[U+(2/3)\ln(8S)]$ in (35) as the total voltage V_t, we can write the asymptotic form of $G(K)$as

$$G(K) = \left(\frac{4}{\ln K}\right)^{1/3}, \qquad K \to \infty. \tag{40}$$

A comparison of the actual data of Morgan and Smits [5] with the asymptotic values as per (40) is shown in Fig. 5, which also contains numerical values computed for linearly graded junctions by the technique described in Section IV. The asymptotic form is found to be an excellent approximation for $K>20$.[2]

Thus, except for very shallow junctions ($a<10^{14}\text{cm}^{-4}$) the asymptotic relation (40) may be used for reverse bias, including zero bias and small forward bias:

$$\frac{LC}{\epsilon} = \left[\frac{S}{-12(U+\frac{2}{3}\ln(8S))}\right]^{1/3}, \tag{41}$$

which in unnormalized form can be written as

$$C^3 = \frac{qa\epsilon^2}{12(V_g - V_a)} \tag{42}$$

where V_g is termed as *gradient voltage* and is given by

$$V_g = \frac{2}{3}\frac{kT}{q}\ln\frac{a^2\epsilon kT/q}{8qn_i^3}, \tag{43}$$

and V_a is the voltage applied to the junction.

Note that the gradient voltage V_a given by (43) is independent of applied voltage, and for a given material at a given temperature it is dependent only on the doping gradient. From the agreement of (40) with numerical values shown in Fig. 5, and the comparison

[2] $K=20$ corresponds to a forward bias of 0.44 V for a junction with $a=10^{20}$ cm^{-4}.

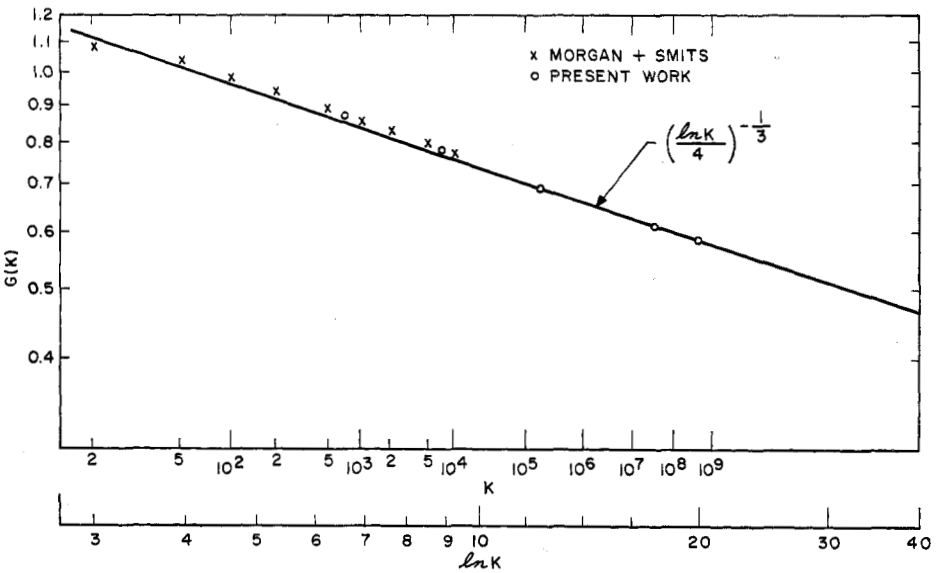

Fig. 5. Comparison of the present work and the asymptotic result (40) with the calculations of Morgan and Smits [3].

of (43) with (5), it can be concluded that for linear-graded junctions the gradient voltage is an excellent approximation to the offset voltage.

A comparison of V_g with the built-in voltage[3] $V_{AA}=(kT/q)\ln(N_1N_2/n_i^2)$ obtained by making the ASCE approximation, where N_1 and N_2 are the impurity concentrations at the edges of the depletion region at zero bias, is shown in Table I for several values of the concentration gradient a.

From Table I it is seen that V_g is of the order of 100 mV smaller than V_{AA}, and that for the lowest concentration gradient considered, the discrepancy in V_{AA} compared to V_g is 37 percent. This could introduce significant errors in calculations of capacitance near zero bias. Nuyts and Van Overstraeten [16] have recently reported that the intercept in numerically computed $1/C^3$ versus V curves is about 0.13 V smaller than V_{AA}. The intercept in their results, however, is not well defined. Detailed calculations show that the offset voltage is a function of the applied voltage, thus causing curvature in a $1/C^3$ versus voltage plot. The intercept formed by drawing a tangent on the curve is therefore dependent on the point considered on the curve. Hence an accurate comparison with their results cannot be made here. Shown in Table II are the computed values of offset voltage as a function of the applied voltage for a junction with $a=10^{22}\text{cm}^{-4}$.

For this junction, the voltage intercept given by Nuyts and Van Overstraeten [16] in their Fig. 2B is about 0.685 V, whereas the gradient voltage is equal to 0.7058 V. Nuyts and Van Overstraeten's intercept value thus agrees with the offset voltage near +0.5 V, whereas the gradient voltage agrees with the offset voltage near 0 V.

[3] This is the quantity Φ_B in Fig. 6.11 of [15].

TABLE I

a (cm^{-4})	V_{AA} (volts)	V_g (volts)
10^{16}	0.3155	0.2296
10^{17}	0.3989	0.3089
10^{18}	0.4815	0.3883
10^{19}	0.5636	0.4677
10^{20}	0.6453	0.5471
10^{21}	0.7267	0.6264
10^{22}	0.8079	0.7058
10^{23}	0.8889	0.7851

TABLE II

Applied Voltage (volts)	Offset Voltage (volts)
+0.5	0.6869
0	0.7065
−0.5	0.7154

VI. Exponential-Constant Doping Profile

Exponential-constant doping profiles, as stated earlier, provide realistic approximations for many diffused p-n junction profiles. Relationships between the characteristic length of this profile and those of Gaussian-constant and error function-constant profiles were given by (15)–(17). A capacitance–voltage relationship for this profile, based on the ASCE approximation, was given by (12). To make this relationship more accurate, we again seek the offset voltage for the profile under consideration. But unlike the results of Section V, it does not appear that an analytical expression approximating the offset voltage can be found by some simple dimensional considerations. We do know, however, that diodes with a very steep diffusion profile should behave like step junctions, while diodes with a very shallow diffusion profile should behave like linearly graded junctions. This is evident from the following computa-

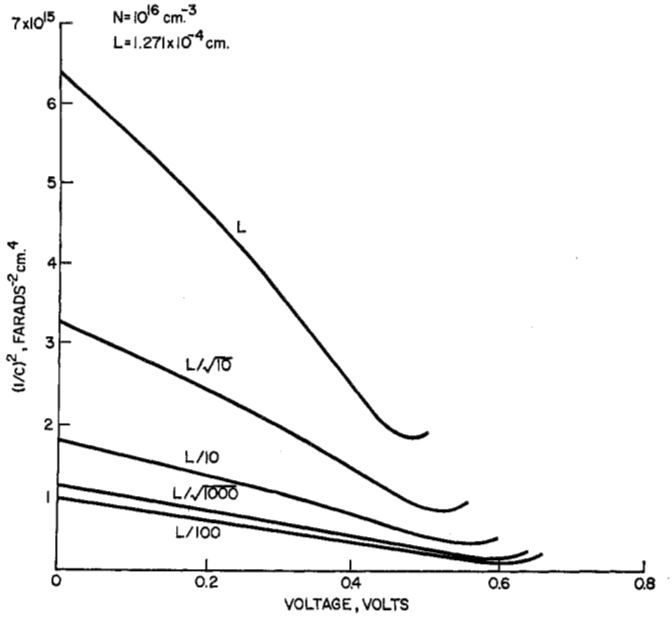

Fig. 6. $1/C^2$ versus applied voltage for diodes with constant background concentration of 10^{16} donors cm^{-3} and varying decay lengths for the superposed exponential profiles of acceptors.

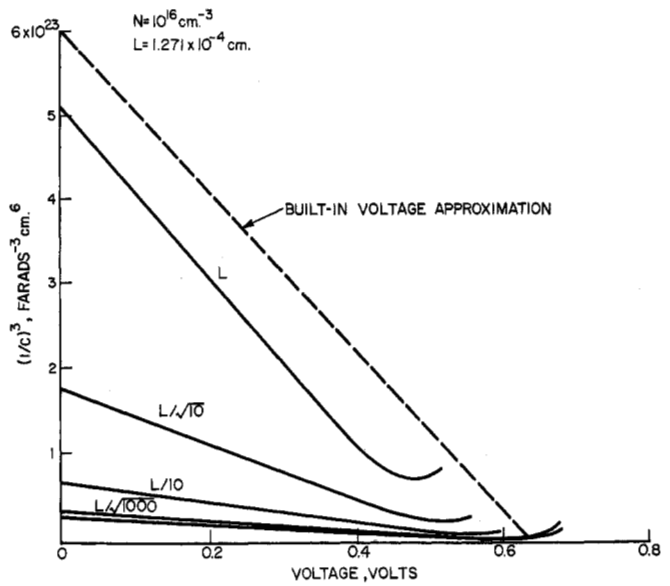

Fig. 7. Same data as in Fig. 6, plotted on a $1/C^3$ versus applied voltage plot.

tions of transition-region capacitance versus voltage, obtained by using the numerical technique of Section IV, for silicon diodes with a background concentration of 10^{16} donors per cm^3 and diffused with acceptor exponential profiles of various characteristic lengths.

Fig. 6 shows the reciprocal squared capacitance as a function of applied voltage for forward bias. The lowest curve for the smallest characteristic length in this figure has a large portion of approximately linear variation with voltage. The slope is very nearly proportional to the inverse of the background donor concentration. This diode is thus similar to a step-junction diode. As we have seen previously, the transition-region capacitance reaches a maximum and then decreases. This is depicted here by a turning up of the curves. Let us now consider the second curve from the top for a more gradual doping transition. On this plot there is some curvature of the same sign as when we plot a linearly graded junction diode on a $1/C^2$ versus V plot. Not shown here is the portion of the curve for large reverse bias. In this range the curve straightens out and eventually reaches the same slope as the lowest curve. The intercept with the voltage axis, after extrapolation, is then much above 1 V.

Let us now see how the same data look on a $1/C^3$ versus voltage plot. Fig. 7 shows this plot. For the most shallow diffusion, the curves have straight line segments, while the curves for steep diffusion have an upward curvature. This curvature, not noticeable here, becomes quite noticeable when the lowest curve is plotted on an expanded scale. Let us now review the concept of built-in voltage in light of these plots. The diode corresponding to the topmost curve has a concentration gradient of 8×10^{19} cm^{-4} at the metallurgical junction. For this the conventional built-in voltage has a value of 0.62 V. Also, with a given concentration gradient, there is an associated slope according to the simple theory based on the ASCE approximation; the line corresponding to this slope and intercept is shown as a dashed line. It is seen that the slope of this line is in good agreement with the slope of the curve obtained by detailed computation. But the intercept of the dashed line is about 100 mV higher than the extrapolated intercept from the computed curve. We recall from Section V that the offset voltage for a linearly graded junction, approximated by the gradient voltage, is also about 100 mV lower than the built-in voltage.

In the following, we give a comprehensive description of the results of accurate numerical calculations, performed by using the techniques of Section IV, for the capacitance of exponential-constant doping profiles. In accordance with the considerations in Section II and III, the format for the representation is chosen as

$$\frac{CL}{\epsilon} = g\left(\frac{SkT/q}{V_0 - V_a}\right) \tag{44}$$

where S, as previously defined, is given by

$$S = \frac{qNL^2}{\epsilon kT/q}$$

and where the major dependence on the applied voltage V_a is provided through the function g, which, as defined in Section III, is the inverse of

$$f(g) = \frac{2g^2}{\coth\left(\frac{1}{2g}\right) - 2g}. \tag{10}$$

Details of the numerical results are represented in (44)

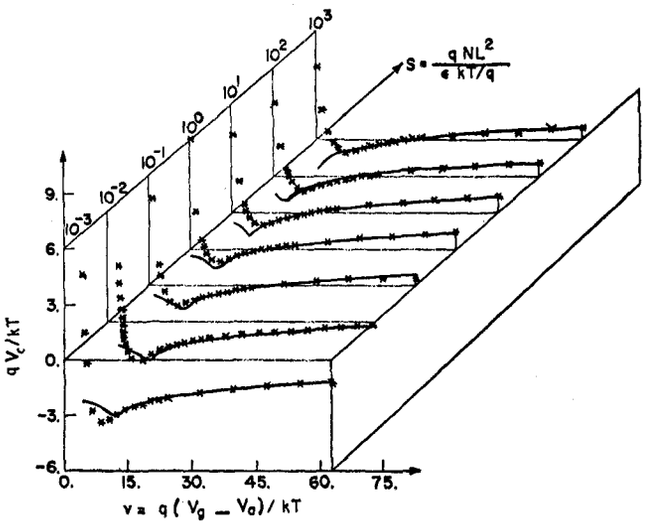

Fig. 8. Numerically computed (asterisks) correction term $V_c(v, S)$, normalized to kT/q, versus v and S for doping parameters of Figs. 6 and 7. The solid lines represent the analytical fit using (46)–(49).

through appropriate adjustment of the offset voltage V_0. As described in Section V, for linearly graded junctions V_0 is approximated by the gradient voltage V_g (43). The numerical results show that for all exponential-constant profiles, the offset voltage (in the region of interest) is within a few kT/q of the gradient voltage corresponding to the doping gradient ($a = N/L$) at the metallurgical junction. Hence, for moderate accuracy the offset voltage can simply be taken as the gradient voltage. Doing so at zero bias, errors of the order of 5 percent or less would be incurred. For improved accuracy we express the offset voltage as the sum of the gradient voltage and a correction term V_c. This correction term depends on applied voltage and doping through the arguments $v = (V_g - V_a)q/kT$ and S:

$$V_0 = V_g + V_c(v, S). \tag{45}$$

Numerically obtained values of the correction term V_c are shown in Fig. 8 as asterisks. The solid lines represent a fit provided by

$$qV_c/kT = \left| v + A \right|^{0.26(1.-0.00033v)} + B \tag{46}$$

where

$$A = -6 + 2\log_{10} S \tag{47}$$

$$B = -0.935(1.614 - P)\exp(-P^2/8.608) - 2.364 \tag{48}$$

with

$$P = \log_{10} S + 3. \tag{49}$$

This fit is reasonably good for $v \geq 7.5$, i.e., for applied voltages 0.2 V below the gradient voltage or less. For $v < 7.5$, although the fit may not be acceptable, it is not very important since in this range the diffusion capacitance begins to dominate over the transition region capacitance. Also note that (46) is free of singularities and hence can be used conveniently in computer-aided circuit analysis.

Equations (44)–(49) are general and apply to any material, provided that the basic assumptions are satisfied, viz., complete ionization and absence of trapping effects. To provide a convenient reference, the capacitance of silicon diodes, as computed by (44)–(49), using the numerical values $n_i = 1.5 \times 10^{15}$ cm^{-3}, $\epsilon = 1.00 \times 10^{-12}$ F/cm, and $kT/q = 0.02585$ V, is shown in Figs. 9–16. These figures show contours of capacitance in the doping parameter space for the following selected values of bias voltages -50, -10, -5, -1, -0.1, 0, 0.1, and 0.2 V. Now, if besides the capacitance and the voltage, the background doping of the material is also given, then the characteristic length for the desired diffusion can be found very simply from these curves. The curves shown in these figures are not extended to the lower left-hand corner, since in this region ($S < 5 \times 10^{-3}$) the fit using (44)–(49) starts losing accuracy. Similar loss of accuracy occurs for $v < 7.5$, and it is reflected in the upper left-hand corner of Figs. 15 and 16.

For determining the doping profile from a pair of C–V measurements, these plots can be used as shown in Fig. 17. Shown here are curves corresponding to measured values of 3.0×10^4pF/cm^2 at 0 V and 1.0×10^4 pF/cm^2 at -10 V. The point of intersection yields $L = 1.25 \times 10^{-5}$cm^{-1} and $N = 1.7 \times 10^{16}$cm^{-3}. If the two capacitances were measured for voltages low enough that the diode is essentially in a linearly graded region, then the corresponding capacitance contours would not intersect, but rather would coincide in the linearly graded region. As is reasonable, in this case only the concentration gradient N/L is revealed by the measurements. Likewise, if the two capacitance values are measured for large reverse bias, the vertical portions of the curves may coincide, and only N but not L is determined.

The above scheme of graphical manipulations is prone to loss of some accuracy besides requiring transparent graphs. To obviate these limitations, we have plotted Figs. 18–21. They may be used to find the doping parameters when capacitance values for one of the following voltage pairs are available: 0, -10 or 0, -1 V. The ordinate in the figures is the capacitance ratio, and the abscissa is the capacitance (per unit area) at the reverse bias. Figs. 20 and 21 contain enlarged sections of Fig. 19. In Fig. 21, the point having an abscissa of 1×10^4pF/cm^2 (capacitance at a bias of -10 V), and an ordinate of 3 (ratio of capacitances at 0 and -10 V) corresponds to the doping parameters of $L = 1.25 \times 10^{-5}$cm and $N = 1.7 \times 10^{16}$cm^{-3}.

The work presented in this paper is applicable for flat, homogeneous junctions. Sidewall effects must be considered separately. Not all of the N–L region of Figs. 9–16 is accessible in conventional measurements because of junction breakdown. Some of the region may be accessible with pulse measurements. Van Overstraeten and DeMan [17] have given curves of breakdown voltage versus the background doping with doping gradient (N/L) as a parameter. For ready

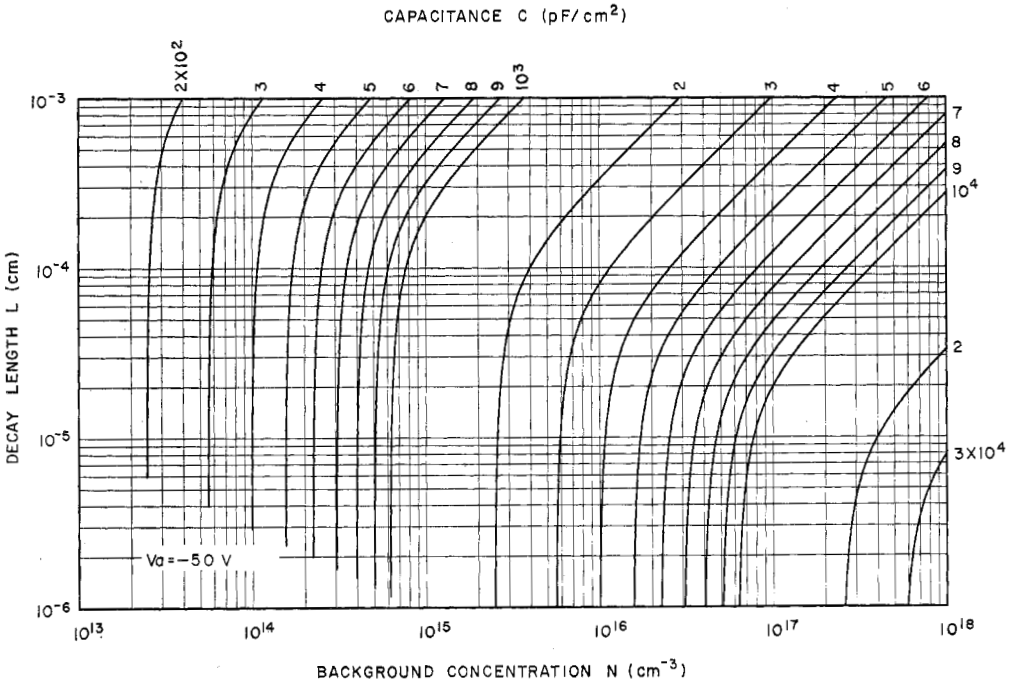

Fig. 9. Contour of constant capacitance in N-L space for -50 V applied to the junction.

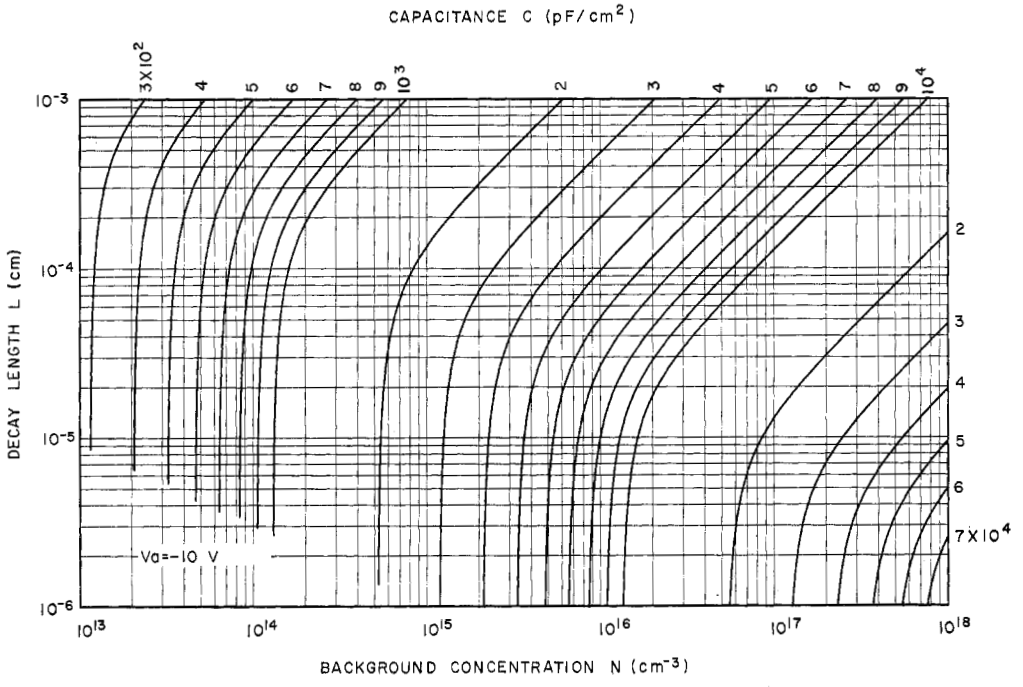

Fig. 10. Contours of constant capacitance in N-L space for -10 V applied to the junction.

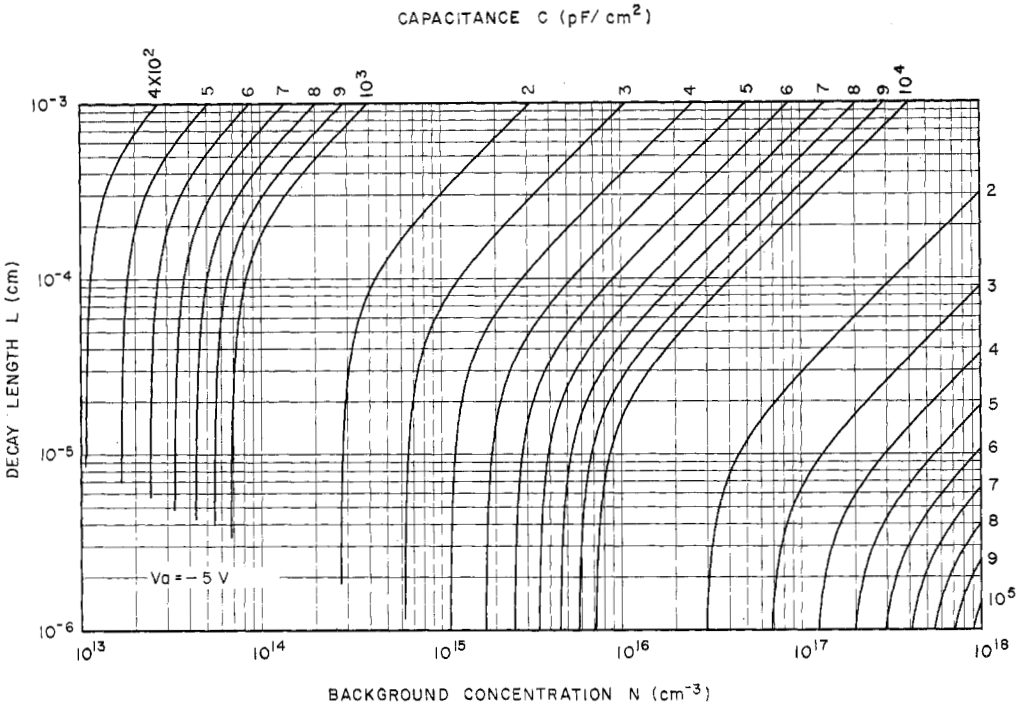

Fig. 11. Contours of constant capacitance in N-L space for -5 V applied to the junction.

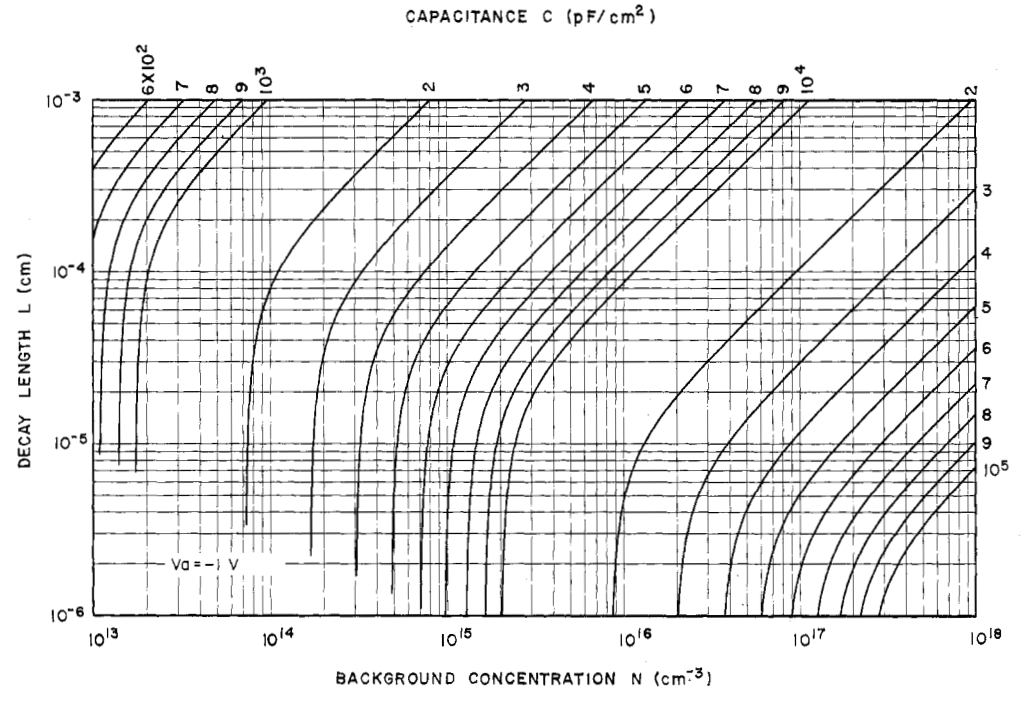

Fig. 12. Contours of constant capacitance in N-L space for -1 V applied to the junction.

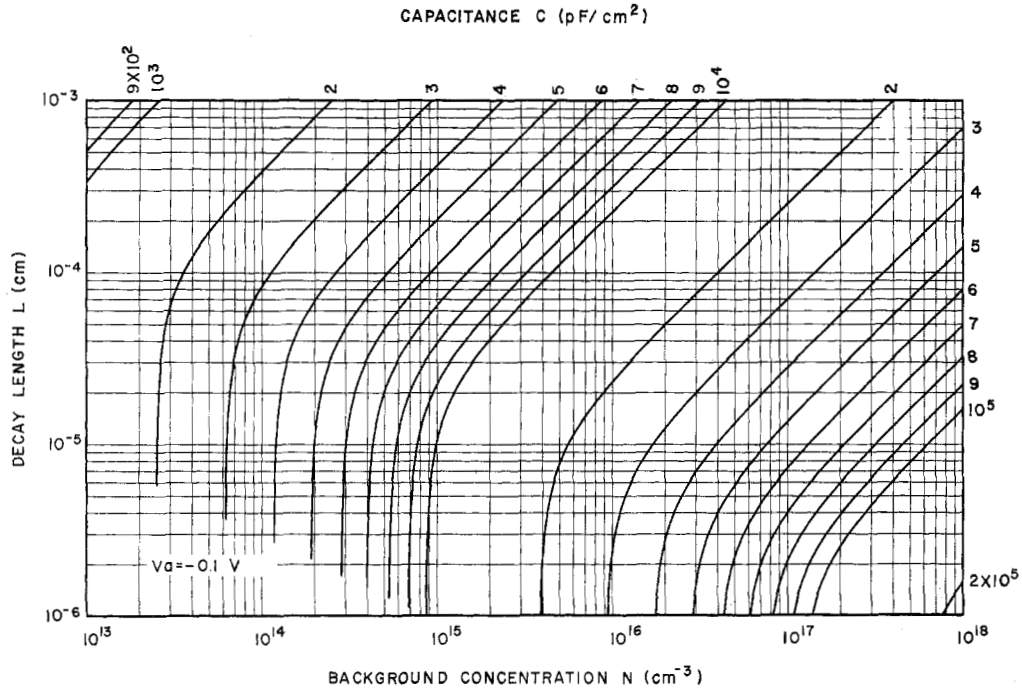

Fig. 13. Contours of constant capacitance in N-L space for -0.1 V applied to the junction.

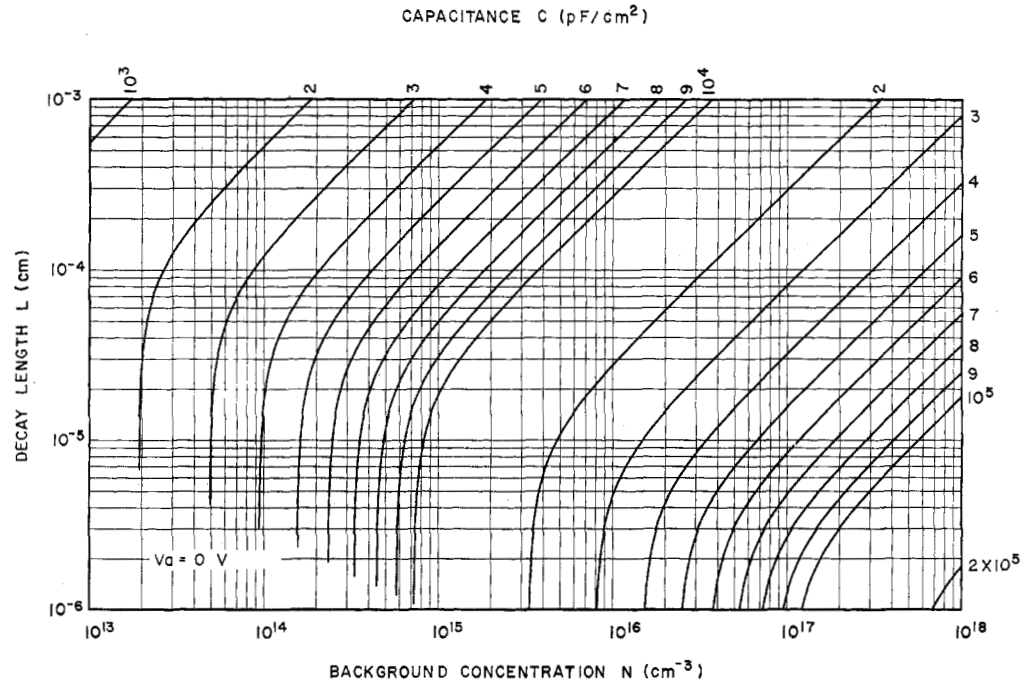

Fig. 14. Contours of constant capacitance in N-L space for 0 V applied to the junction.

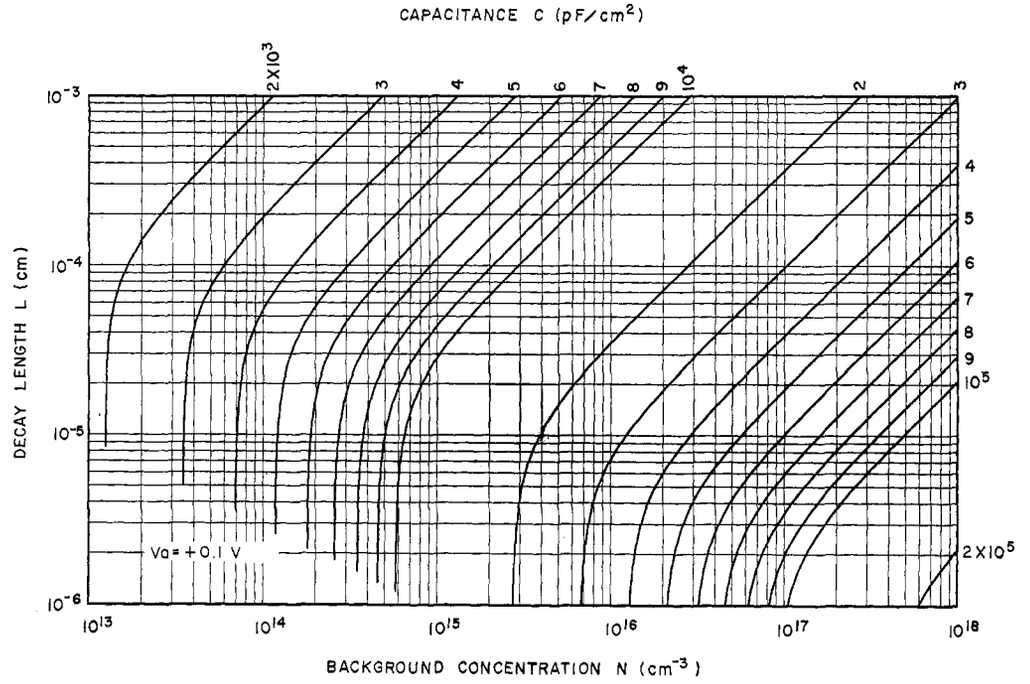

Fig. 15. Contours of constant capacitance in N-L space for 0.1 V applied to the junction.

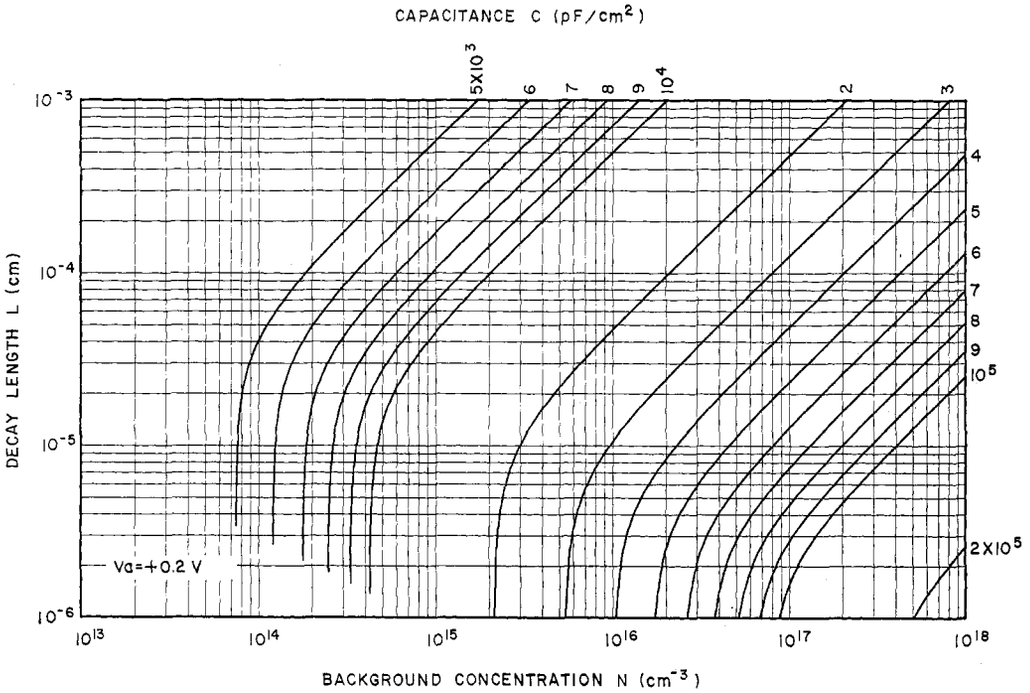

Fig. 16. Contours of constant capacitance in N-L space for 0.2 V applied to the junction.

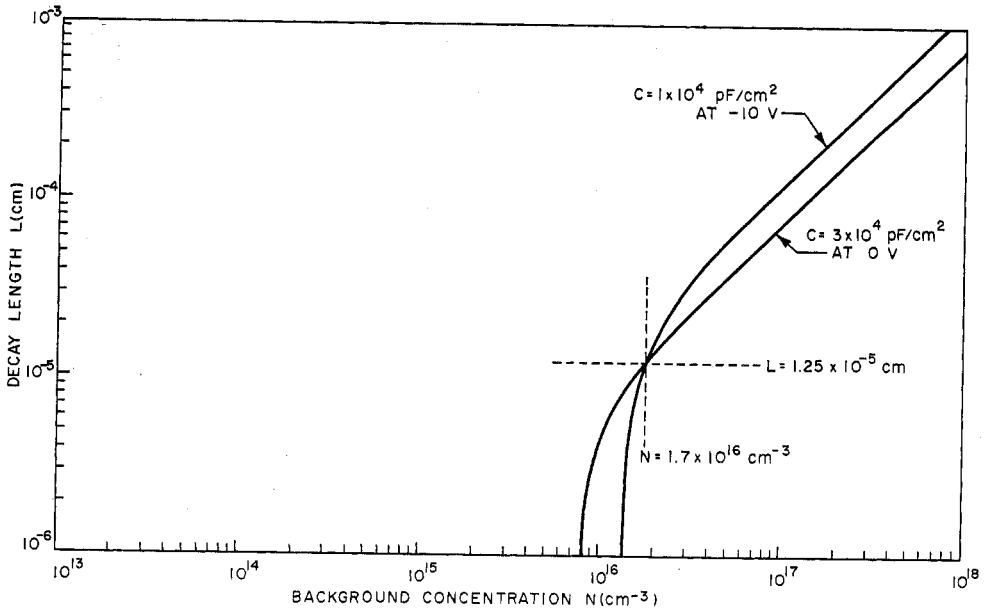

Fig. 17. Use of the contours of constant capacitance at different voltages in determining the doping parameters of a junction.

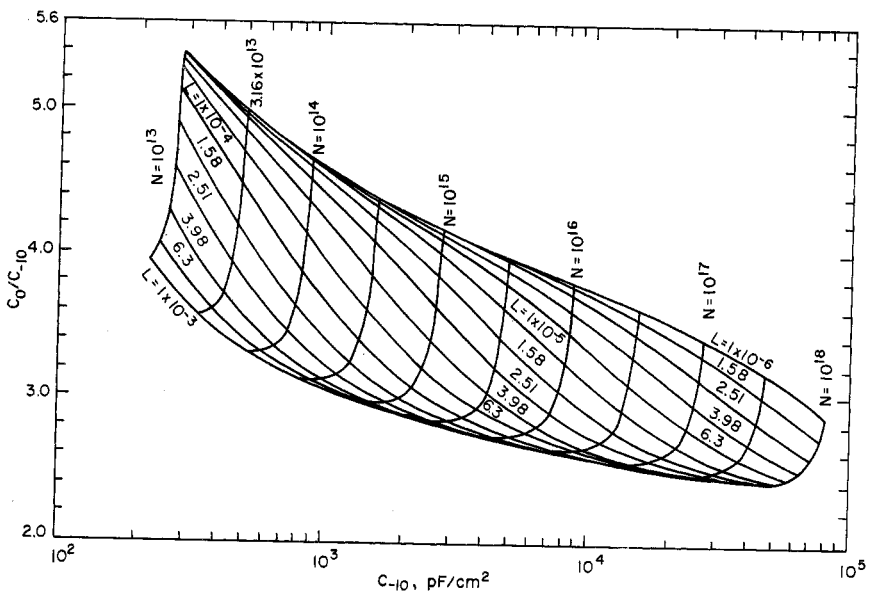

Fig. 18. Contours of constant doping parameters in the space of capacitance at −10 V and the ratio of capacitances at 0 and −10 V.

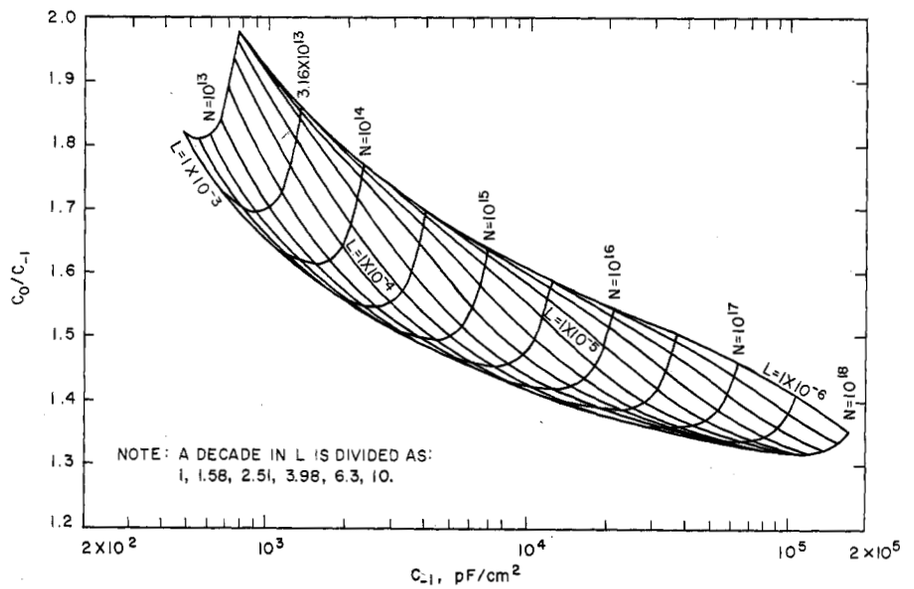

Fig. 19. Contours of constant doping parameters in the space of capacitance at -1 V and the ratio of capacitances at 0 and -1 V.

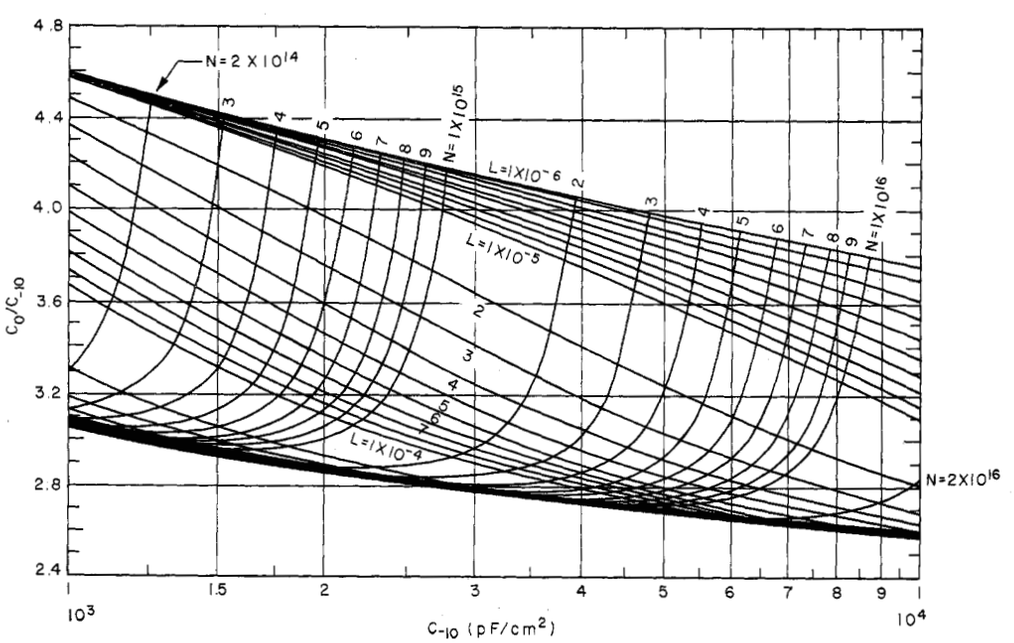

Fig. 20. Portion of Fig. 18 on expanded scale.

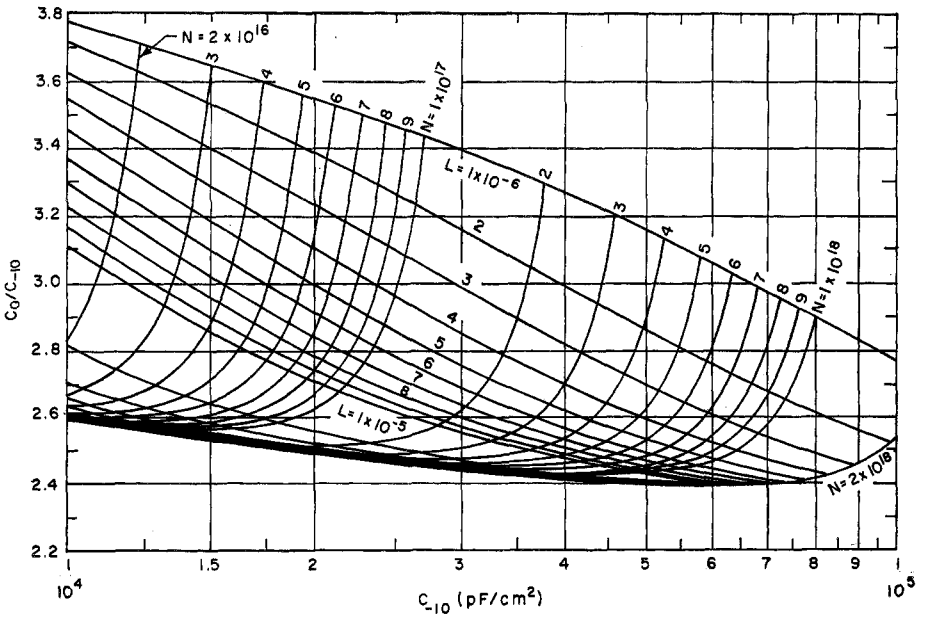

Fig. 21. Portion of Fig. 18 on expanded scale.

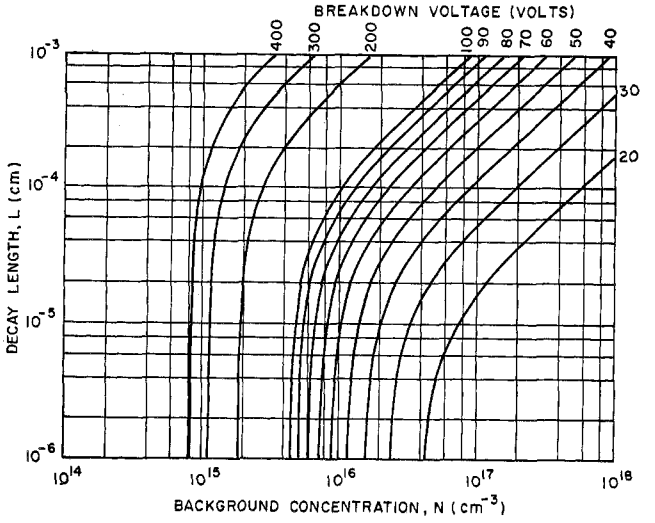

Fig. 22. Contours of constant avalanche breakdown voltage in N-L space.

reference, we have included here the contours of constant breakdown voltage in the $N-L$ plane as shown in Fig. 22. These curves are applicable for flat, homogeneous junctions. The values of avalanche coefficients used in these calculations were taken from Sze and Gibbons [18]. Planar junctions exhibit breakdown lowering due to junction curvature [19], [20].

VII. Summary

In this paper we have attempted to put the capacitance-voltage relationships for p-n junctions on a firm basis. An operational definition of the transition-region capacitance is presented, which facilitates the development of a numerical technique for its computation for any given arbitrary doping profile. Further, the concept of "offset voltage" is developed which lends itself to accurate relationships between capacitance and voltage, and replaces the incorrect usage of the "built-in voltage" near zero bias. For linearly graded junctions, a quantity termed "gradient voltage," derived by some dimensional considerations, is shown to be an excellent approximation for the corresponding offset voltage. For exponential-constant profiles, which form a realistic approximation for many diffused p-n junction profiles, an analytical expression for the offset voltage is found by curve-fitting on the numerically computed values. This expression, being free of singularities and providing accurate $C-V$ relationship near zero bias and into forward bias, is useful for computer-aided circuit analysis and determination or design of doping profiles. The latter is particularly facilitated here by constant capacitance curves in doping parameter space for various applied voltages, and plots of constant parameters for capacitance values at different voltages.

Acknowledgment

The authors wish to thank Mrs. D. M. Stoughton and W. E. Carter for assistance in programming and preparation of figures.

References

[1] J. Hilibrand and R. D. Gold, "Determination of the impurity distribution in junction diodes from capacitance-voltage measurements," *RCA Rev.*, vol. 21, June 1960, pp. 245–252.
[2] H. K. Gummel and D. L. Scharfetter, "Depletion layer capacitance of p$^+$n step junctions," *J. Appl. Phys.*, vol. 38, Apr. 1967, pp. 2148–2153.
[3] Y. F. Chang, "The capacitance of p-n junctions," *Solid-State Electron.*, vol. 10, Apr. 1967, pp. 281–287.
[4] H. P. Kleinknecht, "Space-charge capacitance of asymmetric, abrupt p-n junctions," *J. Appl. Phys.*, vol. 38, June 1967, pp. 3034–3035.
[5] S. P. Morgan and F. M. Smits, "Potential distribution and capacitance of graded p-n junctions," *Bell Syst. Tech. J.*, vol. 39, Nov. 1960, pp. 1573–1602.
[6] C. T. Sah, "Effects of electrons and holes on the transition layer characteristics of linearly graded P-N junctions," *Proc. IRE*, vol. 49, Mar. 1961, pp. 603–618.

[7] D. P. Kennedy and R. R. O'Brien, "On the mathematical theory of the linearly-graded p-n junction," *IBM J. Res. Develop.*, May 1967, pp. 252–270.
[8] H. Lawrence and R. M. Warner, Jr., "Diffused junction depletion layer calculations," *Bell Syst. Tech. J.*, vol. 39, Mar. 1960, pp. 389–404.
[9] T. Misawa, "Impedance of bulk semiconductor in junction diode," *J. Phys. Soc. Jap.*, vol. 12, Aug. 1957, pp. 882–890.
[10] H. K. Gummel, "A self-consistent iterative scheme for one-dimensional steady state transistor calculations," *IEEE Trans. Electron Devices*, vol. ED-11, Oct. 1964, pp. 455–465.
[11] A. DeMari, "An accurate numerical steady-state one-dimensional solution of the *P-N* junction," *Solid-State Electron.*, vol. 11, 1968, pp. 33–58.
[12] H. C. Poon and H. K. Gummel, "Modeling of emitter capacitance," *Proc. IEEE* (Letters), vol. 57, Dec. 1969, pp. 2181–2182.
[13] R. E. Thomas and A. R. Boothroyd, "Estimation of junction depths in double-diffused transistors," *Proc. IEEE* (Letters), vol. 54, Dec. 1966, pp. 1944–1945.
[14] H. N. Ghosh, "A distributed model of the junction transistor and its application in the prediction of the emitter-base diode characteristic, base impedance, and pulse response of the device," *IEEE Trans. Electron Devices*, vol. ED-12, Oct. 1965, pp. 513–531.
[15] A. S. Grove, *Physics and Technology of Semiconductor Devices*. New York: Wiley, 1967.
[16] W. Nuyts and R. J. Van Overstraeten, "Numerical calculations of the capacitance of linearly graded Si p-n junctions," *Electron. Lett.*, vol. 5, Feb. 6, 1969, pp. 54–55.
[17] R. Van Overstraeten and H. DeMan, "Measurement of the ionization rates in diffused silicon p-n junctions," *Solid-State Electron.*, vol. 13, 1970, pp. 583–608.
[18] S. M. Sze and G. Gibbons, "Avalanche breakdown voltages of abrupt and linearly graded p-n junctions in Ge, Si, GaAs, GaP," *Appl. Phys. Lett.*, vol. 8, Mar. 1, 1966, pp. 111–113.
[19] G. Gibbons and J. Kocsis, "Breakdown of voltages of germanium plane-cylindrical junctions," *IEEE Trans. Electron Devices*, vol. ED-12, Apr. 1965, pp. 193–198.
[20] S. M. Sze and G. Gibbons, "Effect of junction curvature on breakdown voltages in semiconductors," *Solid-State Electron.*, vol. 9, 1966, pp. 831–845.
[21] W. Shockley, "The theory of p-n junctions in semiconductors and p-n junction transistors," *Bell Syst. Tech. J.*, vol. 28, 1949, pp. 435–489.

Lumped Modeling of Optical Generation in Nonuniformly Doped Semiconductors

J. STEPHEN BRUGLER, MEMBER, IEEE

Abstract—**When carrier density is normalized and recombination neglected, a single transport element accounts for both drift and diffusion. Optical generation is modeled by discrete current sources, and expressions for lumped elements are obtained in terms of integrals of the doping profile. Good physical intuition with respect to the effect of the profile on photocurrent transport is obtained, and analytical calculation of device quantum efficiency is facilitated.**

I. Introduction

IT IS well known [1], [2] that a drift field caused by an impurity gradient can enhance the collection efficiency of junction photodevices. Exact computation of the effects of such a field on the transport of photogenerated carriers is often quite laborious. In this paper a rather simple approximate lumped model of photogeneration is derived that is both simple and intuitively appealing.

The derivation involves both a change of variable and an approximation. The change of variable is the normalization of excess minority carrier density by its equilibrium value. This use of relative excess minority carrier density leads to a simple model for current transport in nonuniformly doped regions. The approximation is that of negligible bulk recombination. By assuming a diffusion length much greater than the width of the modeled region, the procedure follows the classical analysis of drift transistors [3] in determining the minority carrier density distribution. For thin diffused layers (e.g., a phototransistor base region) the lifetime is generally sufficient for the approximation to be good. As in all lumped models, recombination elements can be added and the number of lumps increased so that the the model approaches the actual distributed minority carrier transport case with arbitrary accuracy.

The minority carrier transport is first analyzed using the relative excess density formulation, and it is shown that a single element accounts for both drift and diffusion. Next, the model is extended to include lumped photocurrent sources. In the subsequent discussion, the relationship of the lumped currents to impurity gradients is considered. Finally, a few illustrative calculations show the utility of the technique.

Manuscript received May 1, 1970; revised October 5, 1970. The work presented in this paper was performed pursuant to Office of Education Grant 0-8-071112-2995. However, the opinions expressed herein do not necessarily reflect the position or policy of the U. S. Office of Education, and no official endorsement should be inferred.
The author is with Stanford University, Stanford, Calif.

II. A Lumped Element for Minority Carrier Transport

The reader is assumed to be familiar with lumped models [4], [5] relating carrier density and current in semiconductor devices under low-level injection conditions. Previous models of transport in nonuniform regions have required two transport elements, one each for drift and diffusion. In this section it is shown that current flow exhibits reciprocity when model port vari-